

# Discontinuous Galerkin Methods on $hp$ -Anisotropic Meshes I: *A Priori* Error Analysis

Emmanuil H. Georgoulis <sup>\*</sup>      Edward Hall <sup>†</sup>      Paul Houston <sup>‡</sup>

November 29, 2006

## Abstract

We consider the *a priori* error analysis of  $hp$ -version interior penalty discontinuous Galerkin methods for second-order partial differential equations with non-negative characteristic form under weak assumptions on the mesh design and the local finite element spaces employed. In particular, we prove *a priori*  $hp$ -error bounds for linear target functionals of the solution, on (possibly) anisotropic computational meshes with anisotropic tensor-product polynomial basis functions. The theoretical results are illustrated by a numerical experiment.

## 1 Introduction

The mathematical modeling of advection, diffusion, and reaction processes arises in many application areas. Typically, the diffusion is small (compared to the magnitude of the advection and/or of the reaction), degenerate, or even vanishes in subregions of the domain of interest, which leads to the development of computationally demanding multi-scale features within the underlying analytical solution; these include boundary/interior layers or even discontinu-

ities in the subregions where the problem is of hyperbolic type. Anisotropically refined meshes aim to be aligned along the domains of definition of such lower-dimensional features of the solution, in order to provide the necessary mesh resolution along the relevant directions, so as to reduce the number of degrees of freedom required to obtain accurate approximate solutions.

Discontinuous Galerkin finite element methods (DGFEMs) exhibit attractive properties for the numerical approximation of problems of hyperbolic or nearly-hyperbolic type, such as local conservation of the state variable and enhanced stability properties in the vicinity of boundary/interior layers and discontinuities present in the analytical solution. Additionally, DGFEMs offer advantages in the context of  $hp$ -adaptivity, such as increased flexibility in the mesh design (irregular grids are admissible) and the freedom of choosing even anisotropic elemental polynomial degrees (i.e., different polynomial degrees in each space direction) without the need to enforce any conformity requirements. Thereby, the combination of DGFEMs, that produce stable approximations even in unresolved regions of the computational domain, and anisotropic mesh refinement, which aims to provide the desired mesh resolution in appropriate spatial directions, is an appealing technique for the numerical approximation of these types of problems.

In this paper and the companion article [8] we develop the error analysis for interior penalty DGFEMs applied to second-order partial differential equations with nonnegative characteristic form on general finite element spaces which are possibly anisotropic in both the local meshsize and the local polynomial

---

<sup>\*</sup>Department of Mathematics, University of Leicester, Leicester LE1 7RH, UK, email: [Emmanuil.Georgoulis@mcs.le.ac.uk](mailto:Emmanuil.Georgoulis@mcs.le.ac.uk).

<sup>†</sup>Department of Mathematics, University of Leicester, Leicester LE1 7RH, UK, email: [ejch1@mcs.le.ac.uk](mailto:ejch1@mcs.le.ac.uk).

<sup>‡</sup>School of Mathematical Sciences, University of Nottingham, University Park, Nottingham NG7 2RD, UK, email: [Paul.Houston@nottingham.ac.uk](mailto:Paul.Houston@nottingham.ac.uk). The research of this author was supported by the EPSRC under grant GR/R76615.

degree. In particular, we shall be concerned with goal-oriented error estimation, whereby the error is measured in terms of a quantity of interest, such as an output or target functional  $J(\cdot)$  of the solution of practical importance. While the companion article [8] will be concerned with the derivation of computable *a posteriori* error bounds, and their implementation within automatic  $hp$ -anisotropic adaptive software, the current paper will focus on *a priori* error estimation. To this end, the proofs of the *a priori* error bounds presented in this article are based on exploiting the analysis developed in [10], which assumed that the underlying computational mesh is shape-regular and that the polynomial approximation orders are isotropic, together with the anisotropic  $hp$ -approximation results presented in [6]; for related work on anisotropic approximation theory, see [1, 3, 4, 7, 15, 16], for example, and the references cited therein. We also refer to the recent article [7], where the goal-oriented error analysis of the interior penalty DGFEM on anisotropic computational meshes, assuming that the polynomial degree is kept fixed, has been developed.

The paper is structured as follows. In Section 2 we introduce the model problem and formulate its discontinuous Galerkin finite element approximation. Section 3 outlines the key approximation results needed for the forthcoming error analysis, based on employing the  $L^2$ -orthogonal projection operator. Then, in Section 4 we develop the *a priori* analysis for the error measured in terms of certain linear target functionals of practical interest. The performance of the  $hp$ -anisotropic DGFEM is then studied in Section 5 through a numerical experiment. Finally, in Section 6 we summarize the work presented in this paper and draw some conclusions.

## 2 Model problem and discretization

We start by first introducing the function spaces that will be used throughout this paper. Given a bounded domain  $\omega$  in  $\mathbb{R}^n$ ,  $n \geq 1$ , we denote by  $H^s(\omega)$  the standard Hilbertian Sobolev space of index  $s \geq 0$  of

real-valued functions defined on  $\omega$ . We set  $L^2(\omega) = H^0(\omega)$ , and denote the  $L^2(\omega)$ -norm by  $\|\cdot\|_\omega$ .

Let  $\Omega$  be a bounded open polyhedral domain in  $\mathbb{R}^d$ ,  $d = 2, 3$ , and let  $\Gamma$  signify the union of its  $(d-1)$ -dimensional open faces. We consider the advection-diffusion-reaction equation

$$\mathcal{L}u \equiv -\nabla \cdot (a \nabla u) + \nabla \cdot (\mathbf{b}u) + cu = f, \quad (1)$$

where  $f \in L^2(\Omega)$  and  $c \in L^\infty(\Omega)$  are real-valued,  $\mathbf{b} = \{b_i\}_{i=1}^d$  is a vector function whose entries  $b_i$  are Lipschitz continuous real-valued functions on  $\bar{\Omega}$ , and  $a = \{a_{ij}\}_{i,j=1}^d$  is a *symmetric* matrix whose entries  $a_{ij}$  are bounded, piecewise continuous real-valued functions defined on  $\bar{\Omega}$ , with

$$\boldsymbol{\zeta}^\top a(\mathbf{x}) \boldsymbol{\zeta} \geq 0 \quad \forall \boldsymbol{\zeta} \in \mathbb{R}^d, \quad \text{a.e. } \mathbf{x} \in \bar{\Omega}. \quad (2)$$

Under this hypothesis, (1) is termed a *partial differential equation with nonnegative characteristic form*. By  $\mathbf{n}(\mathbf{x}) = \{n_i(\mathbf{x})\}_{i=1}^d$  we denote the unit outward normal vector to  $\Gamma$  at  $\mathbf{x} \in \Gamma$ . On introducing the so called *Fichera function*  $\mathbf{b} \cdot \mathbf{n}$  (cf. [17]), we define

$$\begin{aligned} \Gamma_0 &= \{\mathbf{x} \in \Gamma : \mathbf{n}(\mathbf{x})^\top a(\mathbf{x}) \mathbf{n}(\mathbf{x}) > 0\}, \\ \Gamma_- &= \{\mathbf{x} \in \Gamma \setminus \Gamma_0 : \mathbf{b}(\mathbf{x}) \cdot \mathbf{n}(\mathbf{x}) < 0\}, \\ \Gamma_+ &= \{\mathbf{x} \in \Gamma \setminus \Gamma_0 : \mathbf{b}(\mathbf{x}) \cdot \mathbf{n}(\mathbf{x}) \geq 0\}. \end{aligned}$$

The sets  $\Gamma_-$  and  $\Gamma_+$  will be referred to as the inflow and outflow boundary, respectively. Evidently,  $\Gamma = \Gamma_0 \cup \Gamma_- \cup \Gamma_+$ . If  $\Gamma_0$  is nonempty, we shall further divide it into disjoint subsets  $\Gamma_D$  and  $\Gamma_N$  whose union is  $\Gamma_0$ , with  $\Gamma_D$  nonempty and relatively open in  $\Gamma$ . We supplement (1) with the boundary conditions

$$\begin{aligned} u &= g_D \quad \text{on } \Gamma_D \cup \Gamma_-, \\ (a \nabla u) \cdot \mathbf{n} &= g_N \quad \text{on } \Gamma_N, \end{aligned} \quad (3)$$

and adopt the (physically reasonable) hypothesis that  $\mathbf{b} \cdot \mathbf{n} \geq 0$  on  $\Gamma_N$ , whenever  $\Gamma_N$  is nonempty. Additionally, we assume throughout that

$$(c_0(\mathbf{x}))^2 \equiv c(\mathbf{x}) + \frac{1}{2} \nabla \cdot \mathbf{b}(\mathbf{x}) \geq 0 \quad \text{a.e. } \mathbf{x} \in \Omega. \quad (4)$$

For the well-posedness theory (for weak solutions) of the boundary value problem (1), (3), in the case of homogeneous boundary conditions, we refer to [12, 14].

## 2.1 Meshes and finite element spaces

For simplicity of presentation, from this point onwards we assume that  $d = 2$ ; however, we note that all of the results presented in this work naturally generalise to the case  $d = 3$ , by exploiting analogous arguments to those presented in the sequel. Let  $\mathcal{T}$  be a subdivision of the polygonal domain  $\Omega \subset \mathbb{R}^2$  into disjoint open (curvilinear) quadrilateral elements  $\kappa$  constructed via the mappings  $Q_\kappa \circ F_\kappa$ , where  $F_\kappa : \hat{\kappa} := (-1, 1)^2 \rightarrow \tilde{\kappa}$  is an affine mapping of the form

$$F_\kappa(\mathbf{x}) := A_\kappa \mathbf{x} + \vec{b}_\kappa, \quad (5)$$

with  $A_\kappa := \frac{1}{2} \text{diag}(h_1^\kappa, h_2^\kappa)$ , where  $h_1^\kappa$  and  $h_2^\kappa$  are the lengths of the edges of  $\tilde{\kappa}$  parallel to the  $\tilde{x}_1$ - and  $\tilde{x}_2$ -axes, respectively,  $\vec{b}_\kappa$  is a two-component real-valued vector, and  $Q_\kappa : \tilde{\kappa} \rightarrow \kappa$  is a smooth diffeomorphism (cf. Figure 1).

Heuristically, we can say that the affine mapping  $F_\kappa$  defines the size of the element  $\kappa$  and the diffeomorphism  $Q_\kappa$  defines the “shape”. For this reason, we shall be working with diffeomorphisms that are close to the identity in the following sense: the Jacobi matrix  $J_{Q_\kappa}$  of  $Q_\kappa$  satisfies

$$\begin{aligned} C_1^{-1} &\leq \det J_{Q_\kappa} \leq C_1, \\ \|(J_{Q_\kappa})_{ij}\|_{L^\infty(\kappa)} &\leq C_2, \quad i, j = 1, 2 \end{aligned}$$

for all  $\kappa \in \mathcal{T}$  uniformly throughout the mesh for some positive constants  $C_1$  and  $C_2$ .

The above maps are assumed to be constructed so as to ensure that the union of the closures of the disjoint open elements  $\kappa \in \mathcal{T}$  forms a covering of the closure of  $\Omega$ , i.e.,  $\bar{\Omega} = \cup_{\kappa \in \mathcal{T}} \bar{\kappa}$ . We shall restrict ourselves to meshes that are unions of diffeomorphic images of rectangles and to tensor-product polynomial spaces.

Also, we define the *broken Sobolev space* of order  $s$  on an open set  $\Omega$ , subject to a subdivision  $\mathcal{T}$  of  $\Omega$ , as

$$H^s(\Omega, \mathcal{T}) = \{u \in L^2(\Omega) : u|_\kappa \in H^s(\kappa) \quad \forall \kappa \in \mathcal{T}\},$$

together with the corresponding norm.

Let  $\hat{I} \equiv (-1, 1)$  and  $\hat{\kappa} \equiv \hat{I} \times \hat{I} = (-1, 1)^2$ . On the interval  $\hat{I}$  we denote the space of polynomials of degree  $p$  or less by  $\mathcal{P}_p(\hat{I})$ . Then, for  $\vec{p} := (p_1, p_2)$ ,

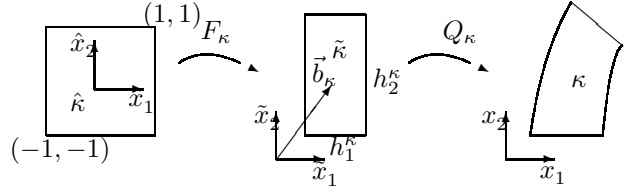


Figure 1: Construction of elements via composition of affine maps and diffeomorphisms.

the *anisotropic tensor-product polynomial space*  $\mathcal{Q}_{\vec{p}}$  on  $\hat{\kappa}$  is defined by  $\mathcal{Q}_{\vec{p}}(\hat{\kappa}) := \mathcal{P}_{p_1}(\hat{I}) \otimes \mathcal{P}_{p_2}(\hat{I})$ , where  $\otimes$  denotes the standard functional tensor product.

Let  $\mathcal{T}$  be a subdivision of the computational domain  $\Omega$  into elements  $\kappa \in \mathcal{T}$  and let  $\mathbf{F} = \{F_\kappa : \kappa \in \mathcal{T}\}$ ,  $\mathbf{Q} = \{Q_\kappa : \kappa \in \mathcal{T}\}$ , where  $F_\kappa, Q_\kappa$  are the maps defined above.

**Definition 2.1** Let  $\vec{p} := (\vec{p}_\kappa : \kappa \in \mathcal{T})$  be the composite polynomial degree vector of the elements in a given subdivision  $\mathcal{T}$ . We define the finite element space with respect to  $\Omega$ ,  $\mathcal{T}$ ,  $\mathbf{F}$ , and  $\vec{p}$  by

$$S_{h, \vec{p}} = \{u \in L^2(\Omega) : u|_\kappa \circ Q_\kappa \circ F_\kappa \in \mathcal{Q}_{\vec{p}_\kappa}(\hat{\kappa})\}.$$

## 2.2 Interior penalty discontinuous Galerkin method

We introduce the (symmetric) interior penalty DGFEM discretization of the advection–diffusion–reaction problem (1), (3). To this end, we introduce the following notation.

An *interior face* of  $\mathcal{T}$  is defined as the (non-empty)  $(d-1)$ -dimensional interior of  $\partial\kappa_i \cap \partial\kappa_j$ , where  $\kappa_i$  and  $\kappa_j$  are two adjacent elements of  $\mathcal{T}$ , not necessarily matching. A *boundary face* of  $\mathcal{T}$  is defined as the (non-empty)  $(d-1)$ -dimensional interior of  $\partial\kappa \cap \Gamma$ , where  $\kappa$  is a boundary element of  $\mathcal{T}$ . We denote by  $\Gamma_{\text{int}}$  the union of all interior faces of  $\mathcal{T}$ . Given a face  $f \subset \Gamma_{\text{int}}$ , shared by the two elements  $\kappa_i$  and  $\kappa_j$ , where the indices  $i$  and  $j$  satisfy  $i > j$ , we write  $\mathbf{n}_f$  to denote the (numbering-dependent) unit normal vector which points from  $\kappa_i$  to  $\kappa_j$ ; on boundary faces, we put  $\mathbf{n}_f = \mathbf{n}$ . Further, for  $v \in H^1(\Omega, \mathcal{T})$  we define the jump of  $v$  across  $f$  and the mean value of  $v$  on  $f$ , respectively, by  $[v] = v|_{\partial\kappa_i \cap f} - v|_{\partial\kappa_j \cap f}$  and  $\langle v \rangle = \frac{1}{2} (v|_{\partial\kappa_i \cap f} + v|_{\partial\kappa_j \cap f})$ .

On a boundary face  $f \subset \partial\kappa$ , we set  $[v] = v|_{\partial\kappa \cap f}$  and  $\langle v \rangle = v|_{\partial\kappa \cap f}$ . Finally, given a function  $v \in H^1(\Omega, \mathcal{T})$  and an element  $\kappa \in \mathcal{T}$ , we denote by  $v_\kappa^+$  (respectively,  $v_\kappa^-$ ) the interior (respectively, exterior) trace of  $v$  defined on  $\partial\kappa$  (respectively,  $\partial\kappa \setminus \Gamma$ ). Since below it will always be clear from the context which element  $\kappa$  in the subdivision  $\mathcal{T}$  the quantities  $v_\kappa^+$  and  $v_\kappa^-$  correspond to, for the sake of notational simplicity we shall suppress the letter  $\kappa$  in the subscript and write, respectively,  $v^+$  and  $v^-$  instead.

Given that  $\kappa$  is an element in the subdivision  $\mathcal{T}$ , we denote by  $\partial\kappa$  the union of  $(d-1)$ -dimensional open faces of  $\kappa$ . Let  $\mathbf{x} \in \partial\kappa$  and suppose that  $\mathbf{n}_\kappa(\mathbf{x})$  denotes the unit outward normal vector to  $\partial\kappa$  at  $\mathbf{x}$ . With these conventions, we define the inflow and outflow parts of  $\partial\kappa$ , respectively, by

$$\begin{aligned}\partial_-\kappa &= \{\mathbf{x} \in \partial\kappa : \mathbf{b}(\mathbf{x}) \cdot \mathbf{n}_\kappa(\mathbf{x}) < 0\}, \\ \partial_+\kappa &= \{\mathbf{x} \in \partial\kappa : \mathbf{b}(\mathbf{x}) \cdot \mathbf{n}_\kappa(\mathbf{x}) \geq 0\}.\end{aligned}$$

For simplicity of presentation, we suppose that the entries of the matrix  $a$  are constant on each element  $\kappa$  in  $\mathcal{T}$ ; *i.e.*,  $a \in [S_{h,0}]_{\text{sym}}^{d \times d}$ . We note that, with minor changes only, our results can easily be extended to the case of  $\sqrt{a} \in [S_{h,q}]_{\text{sym}}^{d \times d}$ ,  $q \geq 0$ ; moreover, for general  $a \in L^\infty(\Omega)_{\text{sym}}^{d \times d}$ , the analysis proceeds in a similar manner, based on employing the modified DG method proposed in [9]. In the following, we write  $\bar{a} = |\sqrt{a}|_2^2$ , where  $|\cdot|_2$  denotes the matrix norm subordinate to the  $l_2$ -vector norm on  $\mathbb{R}^d$  and  $\bar{a}_\kappa = \bar{a}|_\kappa$ .

The DGFEM approximation of (1), (3) is defined as follows: find  $u_{\text{DG}}$  in  $S_{h,\bar{\mathbf{p}}}$  such that

$$B(u_{\text{DG}}, v) = \ell(v) \quad (6)$$

for all  $v \in S_{h,\bar{\mathbf{p}}}$ . Here, the bilinear form  $B(\cdot, \cdot)$  is defined by

$$\begin{aligned}B(w, v) &= B_a(w, v) + B_{\mathbf{b}}(w, v) \\ &\quad - B_f(v, w) - B_f(w, v) + B_\vartheta(w, v),\end{aligned}$$

where

$$B_a(w, v) = \sum_{\kappa \in \mathcal{T}} \int_\kappa a \nabla w \cdot \nabla v \, d\mathbf{x},$$

$$\begin{aligned}B_{\mathbf{b}}(w, v) &= \sum_{\kappa \in \mathcal{T}} \left\{ - \int_\kappa (w \mathbf{b} \cdot \nabla v - c w v) \, d\mathbf{x} \right. \\ &\quad + \int_{\partial_+\kappa} (\mathbf{b} \cdot \mathbf{n}_\kappa) w^+ v^+ \, ds \\ &\quad \left. + \int_{\partial_-\kappa \setminus \Gamma} (\mathbf{b} \cdot \mathbf{n}_\kappa) w^- v^+ \, ds \right\}, \\ B_f(w, v) &= \int_{\Gamma_{\text{int}} \cup \Gamma_{\text{D}}} \langle (a \nabla w) \cdot \mathbf{n}_f \rangle [v] \, ds, \\ B_\vartheta(w, v) &= \int_{\Gamma_{\text{int}} \cup \Gamma_{\text{D}}} \vartheta [w] [v] \, ds,\end{aligned}$$

and the linear functional  $\ell(\cdot)$  is given by

$$\begin{aligned}\ell(v) &= \sum_{\kappa \in \mathcal{T}} \left\{ \int_\kappa f v \, d\mathbf{x} + \int_{\partial\kappa \cap \Gamma_{\text{N}}} g_{\text{N}} v^+ \, ds \right. \\ &\quad - \int_{\partial_-\kappa \cap (\Gamma_{\text{D}} \cup \Gamma_-)} (\mathbf{b} \cdot \mathbf{n}_\kappa) g_{\text{D}} v^+ \, ds \\ &\quad - \int_{\partial\kappa \cap \Gamma_{\text{D}}} g_{\text{D}} ((a \nabla v^+) \cdot \mathbf{n}_\kappa) \, ds \\ &\quad \left. + \int_{\partial\kappa \cap \Gamma_{\text{D}}} \vartheta g_{\text{D}} v^+ \, ds \right\}.\end{aligned}$$

Here  $\vartheta$  is called the *discontinuity-penalization* function and is defined by  $\vartheta|_f = \vartheta_f$  for  $f \subset \Gamma_{\text{int}} \cup \Gamma_{\text{D}}$ , where  $\vartheta_f$  is a nonnegative constant on face  $f$ . The precise choice of  $\vartheta_f$ , which depends on  $a$  and the discretization parameters, will be discussed in detail in the next section. We shall adopt the convention that faces  $f \subset \Gamma_{\text{int}} \cup \Gamma_{\text{D}}$  with  $\vartheta|_f = 0$  are omitted from the integrals appearing in the definition of  $B_\vartheta(w, v)$  and  $\ell_{\text{DG}}(v)$ , although we shall not highlight this explicitly in our notation; the same convention is adopted in the case of integrals where the integrand contains the factor  $1/\vartheta$ .

### 3 $L^2$ -Orthogonal Projection

Before we embark with the error analysis, we present some results taken from [6] regarding the approximation error of the orthogonal  $L^2$ -projection operator onto the finite element space. (All the proofs of the following results can be found in [6].)

Let  $\hat{u} \in L^2(\hat{I})$ , with  $\hat{I} \equiv (-1, 1)$ . We define the  $L^2$ -orthogonal projector  $\hat{\pi}_{\hat{p}}$  on  $\hat{I}$  in a standard fashion by means of truncated Legendre series (see, e.g., [18]). With this definition, for  $\hat{\kappa} \equiv (-1, 1)^2$  we write  $\hat{\Pi}_{\vec{p}} : L^2(\hat{\kappa}) \rightarrow \mathcal{Q}_{\vec{p}}(\hat{\kappa})$ , with composite polynomial degree vector  $\vec{p} = (p_1, p_2)$ , by

$$\hat{\Pi}_{\vec{p}} = \hat{\pi}_{p_1}^1 \hat{\pi}_{p_2}^2 := (\hat{\pi}_{p_1}^1 \otimes I)(I \otimes \hat{\pi}_{p_2}^2),$$

where  $\hat{\pi}_{p_1}^1$  and  $\hat{\pi}_{p_2}^2$  denote the one-dimensional  $L^2$ -projection operators defined above, with the superscripts 1, 2 indicating the directions in which the one-dimensional projectors are applied, respectively, and  $\otimes$  the standard functional tensor product.

**Definition 3.1** Let  $\tilde{u} : \tilde{\kappa} \rightarrow \mathbb{R}$  and  $u : \kappa \rightarrow \mathbb{R}$  and assume that there exist mappings  $F_{\kappa} : \hat{\kappa} \rightarrow \tilde{\kappa}$ ,  $Q_{\kappa} : \tilde{\kappa} \rightarrow \kappa$  as above. We define the  $L^2$ -projection operator  $\tilde{\Pi}_{\vec{p}}$  on  $\tilde{\kappa}$ , with  $\vec{p} = (p_1, p_2)$  being the composite polynomial degree vector, by the relation

$$\tilde{\Pi}_{\vec{p}} \tilde{u} := (\tilde{\Pi}_{\vec{p}}(\tilde{u} \circ F_{\kappa})) \circ F_{\kappa}^{-1}, \quad \text{for } \tilde{u} \in L^2(\tilde{\kappa}),$$

where, as before,  $\tilde{\Pi}_{\vec{p}}$  denotes the  $L^2$ -orthogonal projection onto the reference element  $\tilde{\kappa}$ . Moreover, we define the  $L^2$ -orthogonal projection operator  $\Pi_{\vec{p}}$  on  $\kappa$ , with  $\vec{p} = (p_1, p_2)$ , by

$$\Pi_{\vec{p}} u := (\tilde{\Pi}_{\vec{p}}(u \circ Q_{\kappa})) \circ Q_{\kappa}^{-1}, \quad \text{for } u \in L^2(\kappa).$$

We introduce some notation which we shall use in the approximation estimates below. We define

$$\Phi(p, s, h) := \left( \frac{(p-s)!}{(p+s)!} \right)^2 \left( \frac{h}{2} \right)^{2s}.$$

Let  $J_{Q_{\kappa}} = ((J_{Q_{\kappa}})_{ij})_{i,j=1,2}$  denote the Jacobi matrix of  $Q_{\kappa}$ , which is assumed to be a (smooth) diffeomorphism. In the following approximation estimates for the  $L^2$ -projection error, the generic non-negative constants  $C_{\kappa}$ ,  $C_{\kappa}^1$ , and  $C_{\kappa}^2$ ,  $\kappa \in \mathcal{T}$ , are assumed to be dependent on  $Q_{\kappa}$  but not on the elemental polynomial degree or the affine map  $F_{\kappa}$ . Moreover, we assume that  $C_{\kappa}^1$  and  $C_{\kappa}^2$ ,  $\kappa \in \mathcal{T}$ , are of the form

$$C_{\kappa}^1 := \begin{cases} 1, & \text{if } Q_{\kappa} = \text{id}, \\ C(J_{Q_{\kappa}}), & \text{otherwise,} \end{cases}$$

$$C_{\kappa}^2 := \begin{cases} 0, & \text{if } Q_{\kappa} = \text{id}, \\ C(J_{Q_{\kappa}}), & \text{otherwise,} \end{cases}$$

where  $C(J_{Q_{\kappa}})$  is a generic positive constant depending on  $J_{Q_{\kappa}}$  only. Finally, we define  $\partial \hat{\kappa}_1 := (-1, 1) \times \{\pm 1\}$ ,  $\partial \hat{\kappa}_2 := \{\pm 1\} \times (-1, 1)$ ,  $\partial \hat{\kappa}_i := F_{\kappa}(\partial \hat{\kappa}_i)$  and  $\partial \kappa_i := Q_{\kappa}(\partial \hat{\kappa}_i)$ , for  $i = 1, 2$ .

**Lemma 3.2** Let  $u \in H^{k+1}(\kappa)$ , for  $k \geq 1$ ; then, for  $\tilde{u} := u \circ Q_{\kappa}$ ,  $\vec{p} = (p_1, p_2)$  and  $p_1, p_2 \geq 1$ , we have

$$\|u - \Pi_{\vec{p}} u\|_{\kappa}^2 \leq C_{\kappa} M_{\kappa}^0, \quad (7)$$

where

$$M_{\kappa}^0 := \sum_{i=1}^2 \Phi(p_i, s_i, h_i) \left( \frac{h_i}{2p_i} \right)^2 \|\tilde{\partial}_i^{s_i+1} \tilde{u}\|_{\tilde{\kappa}}^2, \quad (8)$$

and

$$\|\partial_i(u - \Pi_{\vec{p}} u)\|_{\kappa}^2 \leq C_{\kappa}^1 M_{\kappa,i}^1 + C_{\kappa}^2 M_{\kappa,j}^1, \quad (9)$$

with

$$M_{\kappa,i}^1 := p_i \Phi(p_i, s_i, h_i) \|\tilde{\partial}_i^{s_i+1} \tilde{u}\|_{\tilde{\kappa}}^2 + \Phi(p_j, s_j, h_j) \|\tilde{\partial}_j^{s_j} \tilde{\partial}_i \tilde{u}\|_{\tilde{\kappa}}^2, \quad (10)$$

where  $i, j = 1, 2$ ,  $i \neq j$ ,  $0 \leq s_i \leq \min\{p_i, k\}$ , for  $i = 1, 2$ , and  $\tilde{\partial}_i$  is the partial derivative in  $\tilde{x}_i$ -direction in the  $\tilde{x}_1 \tilde{x}_2$ -plane.

**Lemma 3.3** Let  $u \in H^{k+1}(\kappa)$ , with  $k \geq 0$ ; then we have

$$\|u - \Pi_{\vec{p}} u\|_{\partial \kappa_i}^2 \leq C_{\kappa} M_{\partial \kappa,i}^0, \quad (11)$$

where

$$M_{\partial \kappa,i}^0 := \Phi(p_j, s_j, h_j) \frac{h_j}{2p_j} \|\tilde{\partial}_j^{s_j+1} \tilde{u}\|_{\tilde{\kappa}}^2 + \Phi(p_i, s_i, h_i) \frac{h_i}{h_j} \frac{h_i}{2p_i} \|\tilde{\partial}_i^{s_i+1} \tilde{u}\|_{\tilde{\kappa}}^2 + \left( \frac{p_j}{p_i} + 1 \right) \Phi(p_i, s_i, h_i) \frac{h_j}{2p_j} \|\tilde{\partial}_i^{s_i} \tilde{\partial}_j \tilde{u}\|_{\tilde{\kappa}}^2,$$

with  $i, j = 1, 2$ ,  $i \neq j$ ,  $0 \leq s_i \leq \min\{p_i, k\}$ , and  $p_i \geq 1$ , for  $i = 1, 2$ .

**Lemma 3.4** Let  $u \in H^{k+1}(\kappa)$ , with  $k \geq 1$ ; then the following error estimates hold:

$$\|\partial_i(u - \Pi_{\vec{p}} u)\|_{\partial \kappa_i}^2 \leq C_{\kappa}^1 M_{\partial \kappa,i}^1 + C_{\kappa}^2 M_{\partial \kappa,i}^2, \quad (12)$$

$$\|\partial_j(u - \Pi_{\vec{p}} u)\|_{\partial \kappa_i}^2 \leq C_{\kappa}^1 M_{\partial \kappa,i}^2 + C_{\kappa}^2 M_{\partial \kappa,i}^1, \quad (13)$$

with

$$\begin{aligned} M_{\partial\kappa,i}^1 &:= \Phi(p_i, s_i, h_i) \frac{2p_i}{h_i} \left( p_i \frac{h_i}{h_j} \|\tilde{\partial}_i^{s_i+1} \tilde{u}\|_{\tilde{\kappa}}^2 \right. \\ &\quad \left. + \left(1 + \frac{p_i}{p_j}\right) \frac{h_j}{h_i} \|\tilde{\partial}_i^{s_i} \tilde{\partial}_j \tilde{u}\|_{\tilde{\kappa}}^2 \right) \\ &\quad + \Phi(p_j, s_j, h_j) \frac{2p_j}{h_j} \|\tilde{\partial}_j^{s_j} \tilde{\partial}_i \tilde{u}\|_{\tilde{\kappa}}^2, \end{aligned} \quad (14)$$

for  $i, j = 1, 2$ ,  $i \neq j$ ,  $0 \leq s_i \leq \min\{p_i, k\}$ ,  $p_i \geq 1$ ,  $i = 1, 2$ , and

$$\begin{aligned} M_{\partial\kappa,i}^2 &:= p_j^2 \Phi(p_j, s_j, h_j) \frac{2p_j}{h_j} \|\tilde{\partial}_j^{s_j+1} \tilde{u}\|_{\tilde{\kappa}}^2 \\ &\quad + p_j \Phi(p_i, s_i, h_i) \frac{2p_j}{h_j} \|\tilde{\partial}_i^{s_i} \tilde{\partial}_j \tilde{u}\|_{\tilde{\kappa}}^2, \end{aligned} \quad (15)$$

for  $1 \leq s_i \leq \min\{p_i, k\}$ .

## 4 A priori error analysis

The aim of this section is to develop the *a priori* error analysis for general linear target functionals  $J(\cdot)$  of the solution; for related work, we refer to [2, 7, 10], for example.

We begin by defining the *energy norm*  $\|\cdot\|$  by

$$\begin{aligned} \|w\| &:= \left( B_a(w, w) + \|c_0 w\|_{\Omega}^2 \right. \\ &\quad \left. + B_{\vartheta}(w, w) + \frac{1}{2} \|b_n[w]\|_{\Gamma_{\text{int}} \cup \Gamma}^2 \right)^{1/2}, \end{aligned}$$

where  $b_n := \sqrt{|\mathbf{b} \cdot \mathbf{n}_{\kappa}|}$ . We also define the related quantity

$$\begin{aligned} \|[w]\|_{\mu, \nu} &:= \left( \sum_{\kappa \in \mathcal{T}} \left( \mu|_{\kappa} \|\nabla w\|_{\kappa}^2 + \nu|_{\kappa} \|w\|_{\kappa}^2 + \|b_n w\|_{\partial\kappa}^2 \right) \right. \\ &\quad \left. + B_{\vartheta}(w, w) + \|\vartheta^{-1/2} \langle a \nabla w \rangle\|_{L^2(\Gamma_{\text{int}} \cup \Gamma_D)}^2 \right)^{1/2}, \end{aligned}$$

where  $\mu$  and  $\nu$  are non-negative element-wise-constant functions.

We now define the function  $\mathbf{h}$  in  $L^\infty(\Gamma_{\text{int}} \cup \Gamma_D)$ , as  $\mathbf{h}(\mathbf{x}) = \min\{h_j^\kappa, h_j^{\kappa'}\}$ , if  $\mathbf{x}$  is in the interior of  $f = \partial\kappa \cap \partial\kappa'$  for two neighboring elements  $\kappa, \kappa'$  in the mesh  $\mathcal{T}$ , and  $\tilde{f} = Q_{\tilde{\kappa}}^{-1}(f)$  is parallel to the  $\tilde{x}_i$ -axis, for  $i, j = 1, 2$ ,  $i \neq j$ ; we also define  $\mathbf{h}(\mathbf{x}) = h_j^\kappa$ , if  $\mathbf{x}$  is in

the interior of  $f = \partial\kappa \cap \Gamma_D$  and  $\tilde{f} = Q_{\tilde{\kappa}}^{-1}(f)$  is parallel to the  $\tilde{x}_i$ -axis, for  $i, j = 1, 2$ ,  $i \neq j$ . We note that in the isotropic setting we observe that  $\mathbf{h} \sim h$ , where  $h$  denotes the local mesh size. Similarly, we define the function  $\mathbf{p}$  in  $L^\infty(\Gamma_{\text{int}} \cup \Gamma_D)$ , as  $\mathbf{p}(\mathbf{x}) = \max\{p_j^\kappa, p_j^{\kappa'}\}$ , for  $\kappa, \kappa'$  as above; we also write  $\mathbf{p}(\mathbf{x}) = p_j^\kappa$ , if  $\mathbf{x}$  is in the interior of a boundary face as above. Also, we define the function  $\mathbf{a}$  in  $L^\infty(\Gamma_{\text{int}} \cup \Gamma_D)$  by  $\mathbf{a}(\mathbf{x}) = \max\{\bar{a}_\kappa, \bar{a}_{\kappa'}\}$  if  $\mathbf{x}$  is in the interior of  $f = \partial\kappa \cap \partial\kappa'$ , and  $\mathbf{a}(\mathbf{x}) = \bar{a}_\kappa$  if  $\mathbf{x}$  is in the interior of  $\partial\kappa \cap \Gamma_D$ .

With this notation, we now provide the following coercivity result for the bilinear form  $B(\cdot, \cdot)$  over  $S_{h, \bar{\mathbf{p}}} \times S_{h, \bar{\mathbf{p}}}$ .

**Theorem 4.1** *Define the discontinuity-penalization parameter  $\vartheta$  arising in (6) by*

$$\vartheta|_f \equiv \vartheta_f = C_\vartheta \frac{\mathbf{ap}^2}{\mathbf{h}} \quad \text{for } f \subset \Gamma_{\text{int}} \cup \Gamma_D, \quad (16)$$

where  $C_\vartheta$  is a sufficiently large positive constant (see Remark 4.2 below). Then, there exists a positive constant  $C$ , which depends only on the dimension  $d$ , such that

$$B(v, v) \geq C \|v\|^2 \quad \forall v \in S_{h, \bar{\mathbf{p}}}. \quad (17)$$

**Remark 4.2** *Theorem 4.1 indicates that the DG scheme is coercive over  $S_{h, \bar{\mathbf{p}}} \times S_{h, \bar{\mathbf{p}}}$  provided that the constant  $C_\vartheta > 0$  arising in the definition of the discontinuity-penalization parameter  $\vartheta$ , is chosen sufficiently large (see, e.g., [5] for details).*

For the proceeding error analysis, we assume that the solution  $u$  to the boundary value problem (1), (3) is sufficiently smooth: namely,  $u \in H^{3/2+\varepsilon}(\Omega, T)$ ,  $\varepsilon > 0$ , and the functions  $u$  and  $(a \nabla u) \cdot \mathbf{n}_f$  are continuous across each face  $f \subset \partial\kappa \setminus \Gamma$  that intersects the subdomain of ellipticity,  $\Omega_a = \{\mathbf{x} \in \bar{\Omega} : \boldsymbol{\zeta}^\top a(\mathbf{x}) \boldsymbol{\zeta} > 0 \ \forall \boldsymbol{\zeta} \in \mathbb{R}^d\}$ . If this smoothness requirement is violated, the discretization method has to be modified accordingly, cf. [12]. We note that under these assumptions, the following Galerkin orthogonality property holds:

$$B_{\text{DG}}(u - u_{\text{DG}}, v) = 0 \quad \forall v \in S_{h, \bar{\mathbf{p}}}. \quad (18)$$

For simplicity of presentation, it will be assumed in the proceeding analysis, that the velocity vector  $\mathbf{b}$  satisfies the following assumption:

$$\mathbf{b} \cdot \nabla_{\mathcal{T}} v \in S_{h,\bar{\mathbf{p}}} \quad \forall v \in S_{h,\bar{\mathbf{p}}}, \quad (19)$$

where  $\nabla_{\mathcal{T}} v$  denotes the broken gradient of  $v$ , defined elementwise. To ensure that (1) is then meaningful (i.e., that the characteristic curves of the differential operator  $\mathcal{L}$  are correctly defined), we still assume that  $\mathbf{b} \in [W_{\infty}^1(\Omega)]^d$ .

The choice of the  $L^2$ -projection operator is essential in the following *a priori* error analysis, in order to ensure that

$$(u - \Pi_{\bar{\mathbf{p}}} u, \mathbf{b} \cdot \nabla_{\mathcal{T}} v) = 0 \quad (20)$$

for all  $v$  in  $S_{h,\bar{\mathbf{p}}}$ , where  $(\cdot, \cdot)$  denotes the  $L^2(\Omega)$  inner product (cf. the proofs of Lemma 4.4 and Theorem 4.5 below).

**Remark 4.3** *Hypothesis (19) is a standard condition assumed for the analysis of the hp-version of the DGFEM; see, for example, [6, 10, 12]. Indeed, this condition is essential for the derivation of a priori error bounds for the advection part of the partial differential operator  $\mathcal{L}$  which are optimal in both the mesh size  $h$  and spectral order  $p$ ; in the absence of this assumption, optimal  $h$ -convergence bounds may still be derived, though a loss of  $p^{1/2}$  is observed in the resulting error analysis (cf. [12] for the shape-regular case and [5] (Chapter 5) for the anisotropic case), unless the scheme (6) is supplemented by appropriate streamline-diffusion stabilization, cf. [11].*

We shall now derive the *a priori* error bound for the interior penalty DGFEM introduced in Section 2.2. To this end, we decompose the global error  $u - u_{\text{DG}}$  as

$$u - u_{\text{DG}} = (u - \Pi_{\bar{\mathbf{p}}} u) + (\Pi_{\bar{\mathbf{p}}} u - u_{\text{DG}}) \equiv \eta + \xi, \quad (21)$$

where  $\Pi_{\bar{\mathbf{p}}}$  denotes the  $L^2$ -projection operator introduced in Section 3. With these definitions we have the following result.

**Lemma 4.4** *Assume that (4) and (19) hold and let  $\gamma_1|_{\kappa} = \|c/c_0\|_{L^{\infty}(\kappa)}^2$ ; then the functions  $\xi$  and  $\eta$  defined by (21) satisfy the following inequality*

$$|||\xi||| \leq C[|\eta|]_{\mathbf{a},\gamma_1}, \quad (22)$$

where  $C$  is a positive constant that depends only on the dimension  $d$ .

**Proof.** From the Galerkin orthogonality condition (18), we deduce that  $B_{\text{DG}}(\xi, \xi) = -B_{\text{DG}}(\eta, \xi)$ , where  $\xi$  and  $\eta$  are as defined in (21). Thereby, employing the coercivity result stated in Theorem 4.1, gives

$$|||\xi|||^2 \leq -\frac{1}{C} B_{\text{DG}}(\eta, \xi). \quad (23)$$

Using the identity (20), and successive continuous and discrete versions of the Cauchy-Schwarz inequality, the right-hand side of (23) may be bounded as follows:

$$B_{\text{DG}}(\eta, \xi) \leq C |||\xi||| [|\eta|]_{\mathbf{a},\gamma_1}; \quad (24)$$

see [19] for details (cf., also [12]). On substituting (24) into (23) we obtain the desired result.  $\square$

The proof of the forthcoming *a priori* error bound rests on exploiting a duality argument. To this end, we introduce the following *dual* or *adjoint* problem: find  $z \in H^2(\Omega, \mathcal{T})$  such that

$$B(w, z) = J(w) \quad \forall w \in H^2(\Omega, \mathcal{T}). \quad (25)$$

Let us assume that (25) possesses a unique solution. Clearly, the validity of this assumption depends on the choice of the linear functional under consideration; cf. the discussion in [13].

For the rest of this section, let us now assume that the following *bounded local variation conditions* hold for the mesh parameters, i.e., there exist  $\rho_i$  and  $\delta_i$ ,  $i = 1, 2$ , such that  $\rho_i^{-1} \leq p_i^{\kappa}/p_i^{\kappa'} \leq \rho_i$  and  $\delta_i^{-1} \leq h_i^{\kappa}/h_i^{\kappa'} \leq \delta_i$ ,  $i = 1, 2$ , for all pairs of neighbouring elements  $\kappa, \kappa' \in \mathcal{T}$ . Finally we assume that the subdivision  $\mathcal{T}$  is 1-irregular (see [12] for details).

With these hypotheses, we now proceed to prove the main result of this section.

**Theorem 4.5** *Let  $\Omega \subset \mathbb{R}^2$  be a bounded polyhedral domain,  $\mathcal{T} = \{\kappa\}$  a 1-irregular subdivision of  $\Omega$ ,*

such that the mesh parameters satisfy the bounded local variation conditions. Then, assuming that conditions (4) and (19) hold, and  $u \in H^k(\Omega, \mathcal{T})$ ,  $k \geq 2$ ,  $z \in H^l(\Omega, \mathcal{T})$ ,  $l \geq 2$ , then the solution  $u_{\text{DG}} \in S_{h,\bar{\mathbf{p}}}$  of (6) obeys the error bound

$$\begin{aligned} & |J(u) - J(u_{\text{DG}})|^2 \\ & \leq C \left( \sum_{\kappa \in \mathcal{T}} \sum_{i=1}^2 \Phi(p_i^\kappa, s_i^\kappa, h_i^\kappa) \max_{(m,n) \in A} \left\{ \left( \frac{p_j^\kappa}{p_i^\kappa} \right)^m \left( \frac{h_i^\kappa}{h_j^\kappa} \right)^n \right\} \right. \\ & \quad \times (\alpha_\kappa p_i^\kappa + h_i^\kappa \beta_2 + \left( \frac{h_i^\kappa}{p_i^\kappa} \right)^2 (\beta_1 + \gamma_1)) |u|_{t_{i+1,\kappa,i}}^2 \\ & \quad \times \left( \sum_{\kappa \in \mathcal{T}} \sum_{i=1}^2 \Phi(p_i^\kappa, s_i^\kappa, h_i^\kappa) \max_{(m,n) \in A} \left\{ \left( \frac{p_j^\kappa}{p_i^\kappa} \right)^m \left( \frac{h_i^\kappa}{h_j^\kappa} \right)^n \right\} \right. \\ & \quad \times (\alpha_\kappa p_i^\kappa + h_i^\kappa \beta_2 + \left( \frac{h_i^\kappa}{p_i^\kappa} \right)^2 (\beta_1 + \gamma_2)) |z|_{t_{i+1,\kappa,i}}^2 \Big), \end{aligned} \quad (26)$$

with  $A = \{(0,0), (0,1), (0,2), (-1,0), (1,2), (2,2)\}$ , and

$$|w|_{r,\kappa,i} := \left( \|\tilde{\partial}_i^r \tilde{w}\|_{\tilde{\kappa}}^2 + \left( \frac{h_j^\kappa}{h_i^\kappa} \right)^2 \|\tilde{\partial}_i^{r-1} \tilde{\partial}_j \tilde{w}\|_{\tilde{\kappa}}^2 \right)^{1/2},$$

for  $2 \leq s_i^\kappa \leq \min(p_i^\kappa + 1, k)$  and  $2 \leq t_i^\kappa \leq \min(p_i^\kappa + 1, l)$ , where  $\alpha|_\kappa = \bar{a}_\kappa$ ,  $\beta_1|_\kappa = \|c + \nabla \cdot \mathbf{b}\|_{L^\infty(\kappa)}$ ,  $\beta_2|_\kappa = \|\mathbf{b}\|_{L^\infty(\kappa)}$ ,  $\gamma_1|_\kappa = \|c/c_0\|_{L^\infty(\kappa)}$ ,  $\gamma_2|_\kappa = \|(c + \nabla \cdot \mathbf{b})/c_0\|_{L^\infty(\kappa)}^2$  for all  $\kappa \in \mathcal{T}$ . Here,  $C$  is a constant independent on the mesh parameters and the data.

**Proof.** Decomposing the error  $u - u_{\text{DG}}$  as in (21), we note that the error in the target functional  $J(\cdot)$  may be expressed as follows:

$$\begin{aligned} J(u) - J(u_{\text{DG}}) &= B(\eta, z - z_{h,p}) + B(\xi, z - z_{h,p}) \\ &\equiv \text{I} + \text{II}, \end{aligned} \quad (27)$$

for any  $z_{h,p} \in S_{h,\bar{\mathbf{p}}}$ . Let us first deal with term I. To this end, we define  $z_{h,p} = \Pi_{\bar{\mathbf{p}}} z$  and  $w = z - z_{h,p}$ ; after a lengthy, but straightforward calculation, we deduce that

$$|\text{I}| \leq C[\|\eta\|_{\mathbf{a}+\beta_2\epsilon^{-1},\beta_1}][w]_{\mathbf{a},\beta_1+\beta_2\epsilon}, \quad (28)$$

for any real positive element-wise constant function  $\epsilon$  (whose precise definition is currently at our disposal). Let us now consider term II. Here, we note that a

bound analogous to (24) in the proof of Lemma 4.4 holds with  $\eta$  and  $\xi$  replaced by  $\xi$  and  $w = z - z_{h,p}$  in (24), respectively. Indeed, in this case we have that

$$|\text{II}| = |B_{\text{DG}}(\xi, w)| \leq C[\|\xi\|][w]_{\mathbf{a},\gamma_2}. \quad (29)$$

Thereby, employing Lemma 4.4 in (29) and inserting the result and (28) into (27) we deduce that

$$\begin{aligned} & |J(u) - J(u_{\text{DG}})| \\ & \leq C[\|\eta\|_{\mathbf{a}+\beta_2\epsilon^{-1},\beta_1+\gamma_1}][w]_{\mathbf{a},\beta_1+\beta_2\epsilon+\gamma_2}. \end{aligned} \quad (30)$$

Selecting  $\epsilon|_\kappa = \max_{i=1,2}\{p_i^\kappa/h_i^\kappa\}$ , employing the definition of the discontinuity-penalization parameter  $\vartheta$  stated in (16), together with the bounded variation conditions, and applying the approximation results from Section 3, the result follows after rearranging the terms involved.  $\square$

**Remark 4.6** The above result represents an extension of the a priori error bounds derived in the articles [7, 10] to the case when general anisotropic computational meshes are employed and anisotropic local polynomial degrees are allowed.

**Remark 4.7** Upon application of Stirling's formula for the factorials arising in the definition of  $\Phi$ , it can be shown that the error estimate stated in Theorem 4.5 is  $h$ -optimal and slightly  $p$ -suboptimal (by one order of  $p$ ). This is in complete agreement with the results presented for the isotropic case in [10].

When the analytical solution of both the primal and the dual problems is sufficiently smooth, then it can be shown that the error converges to zero at an exponential rate with respect to the local (directional) polynomial degrees. More precisely, we have the following result.

**Corollary 4.8** Let  $\Omega \subset \mathbb{R}^2$  be a bounded polyhedral domain,  $\mathcal{T} = \{\kappa\}$  a 1-irregular subdivision of  $\Omega$ , such that the mesh parameters satisfy the bounded local variation conditions. Then, assuming that conditions (4) and (19) hold, and that  $u, z$  are analytic functions on a neighbourhood of  $\Omega$ , the solution  $u_{\text{DG}} \in S_{h,\bar{\mathbf{p}}}$  of (6) obeys the error bound

$$\begin{aligned} & |J(u) - J(u_{\text{DG}})|^2 \leq C(\alpha, \beta_1, \beta_2, \gamma_1, \gamma_2) \\ & \times \left( \sum_{\kappa \in \mathcal{T}} \sum_{i=1}^2 e^{-r_i p_i^\kappa} N_i^\kappa \right) \left( \sum_{\kappa \in \mathcal{T}} \sum_{i=1}^2 e^{-q_i p_i^\kappa} N_i^\kappa \right), \end{aligned} \quad (31)$$



where

$$N_i^\kappa := (h_i^\kappa)^{2s_i^\kappa} |\tilde{\kappa}| \max_{(m,n) \in A} \left\{ (p_i^\kappa)^{4-m} (p_j^\kappa)^m \left( \frac{h_i^\kappa}{h_j^\kappa} \right)^n \right\},$$

$r_i, q_i$  are positive constants depending on the domain of analyticity of  $u$  and  $z$ , respectively, and  $|\cdot|$  denotes the two-dimensional Lebesgue measure of a (measurable) subset of  $\Omega$ ; the set  $A$  and the data-related constants  $\alpha, \beta_1, \beta_2, \gamma_1$ , and  $\gamma_2$  are as in the statement of Theorem 4.5.

**Proof.** The proof follows by combining the estimate in Theorem 4.5 together with Lemma 7.17 from [6].  $\square$

The *a priori* bound stated in Theorem 4.5 clearly highlights that in order to minimize the error in the computed target functional  $J(\cdot)$ , the design of an optimal mesh must exploit anisotropic information emanating from both the primal and dual solutions  $u$  and  $z$ , respectively. Indeed, a mesh solely optimized for  $u$  may be completely inappropriate for  $z$ , and vice versa, thus there must be a trade-off between aligning the elements with respect to either solution in order to minimize the overall error in  $J(\cdot)$ .

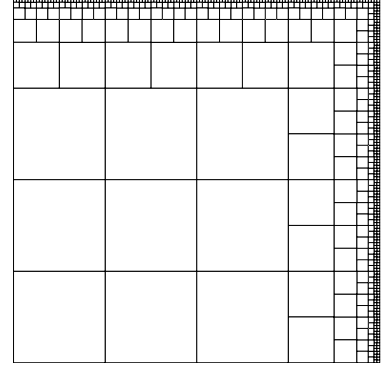
## 5 Numerical experiment

In this section we present a numerical example to highlight the practical performance of the DGFEM on a sequence of *a priori* designed anisotropic  $hp$ -refined computational meshes. To this end, we consider the following singularly perturbed advection-diffusion problem equation  $-\varepsilon \Delta u + u_x + u_y = f$ , for  $(x, y) \in (0, 1)^2$ , where  $0 < \varepsilon \ll 1$  and  $f$  is chosen so that

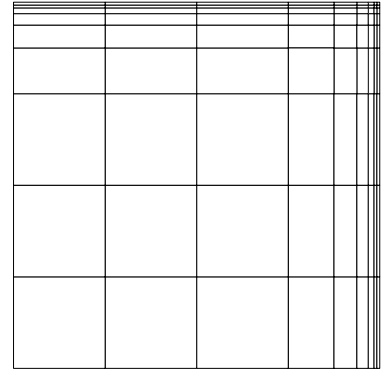
$$u(x, y) = x + y(1 - x) + [e^{-1/\varepsilon} - e^{-(1-x)(1-y)/\varepsilon}] [1 - e^{-1/\varepsilon}]^{-1}, \quad (32)$$

cf. [12]. For  $0 < \varepsilon \ll 1$  the solution (32) has boundary layers along  $x = 1$  and  $y = 1$ . Here, we suppose that the aim of the computation is to calculate the value of the (weighted) mean-value of  $u$  over the computational domain  $\Omega$ , i.e.,

$$J(u) = \int_{\Omega} u \psi \, d\mathbf{x},$$



(a)



(b)

Figure 2: (a) Isotropically refined mesh employed for  $\varepsilon = 10^{-3}$ , with 745 elements; (b) Anisotropically refined mesh employed for  $\varepsilon = 10^{-3}$ , with 81 elements.

where the weight function  $\psi$  is chosen so that

$$z(x, y) = 4y(1 - y)(1 - e^{-\alpha(1-x)} - (1 - e^{-\alpha})(1 - x));$$

setting  $\alpha = 100$  gives rise to a strong boundary layer along the boundary  $x = 1$ ,  $0 \leq y \leq 1$ , cf. [4].

Here, we consider a sequence of  $hp$ -finite element spaces employing a combination of isotropically/anisotropically refined computational meshes with isotropic/anisotropic polynomial degrees. More precisely, starting from a uniform  $5 \times 5$  square mesh, we first perform  $n$ ,  $n \geq 0$ , isotropic or anisotropic refinements of this initial mesh in order to capture the boundary layers present within the underlying primal solution  $u$ . Here, only elements which lie on the

right-hand side or top boundaries of  $\Omega$  are refined; Figure 2 shows the two types of meshes generated by this algorithm with  $n = 5$ . Once the mesh has been refined, this is then kept fixed, and the polynomial degrees are either uniformly (isotropically) increased, or anisotropically refined using the following strategy: at each step of the algorithm, the polynomial degrees for *all* elements are increased in the  $y$ -direction by 1, while those in the  $x$ -direction are increased by 2. This latter strategy is motivated by the fact that the dual solution  $z$  only has anisotropy in the  $x$ -direction. We remark that these  $hp$ -meshes are designed purely on the basis of *a priori* considerations, are not expected to be optimal, but are constructed merely to demonstrate the potential benefits of employing anisotropic  $hp$ -mesh refinement. Indeed, given the structure of the dual solution  $z$ , one may well expect that the computational mesh may be less refined in the region containing the boundary layer along  $y = 1$  present in the primal solution  $u$ .

In Figures 3, 4, & 5 we plot the (square root) of the degrees of freedom employed in the finite element space  $S_{h,\bar{p}}$  against the error in the computed target functional  $J(\cdot)$ , for  $\varepsilon = 10^{-2}, 10^{-3}, 10^{-4}$ , respectively, using each of the four refined  $hp$ -mesh distributions defined above, namely: isotropic  $h$  and isotropic  $p$ , isotropic  $h$  and anisotropic  $p$ , anisotropic  $h$  and isotropic  $p$ , anisotropic  $h$  and anisotropic  $p$ . Here, we have selected  $n = 2, 5, 8$  for  $\varepsilon = 10^{-2}, 10^{-3}, 10^{-4}$ , respectively. Firstly, we note that in all cases, the convergence lines are (on average) straight, indicating exponential rates of convergence have been achieved using all four refinement strategies for each  $\varepsilon$ , which is in agreement with Corollary 4.8. Secondly, for each  $\varepsilon$  we observe that the computed error, for a given number of degrees of freedom, employing the isotropic  $h$  and isotropic  $p$  strategy is always inferior to the algorithm employing isotropic  $h$  and anisotropic  $p$ . Similarly, this latter strategy is inferior to exploiting anisotropic  $h$  and isotropic  $p$ , which is in turn inferior to the use of anisotropic  $h$  and anisotropic  $p$ -refinement. Indeed, here we observe that the use of an anisotropically refined starting mesh yields a vast improvement in the computed error, for a given number of degrees of freedom, in comparison to standard isotropic refine-

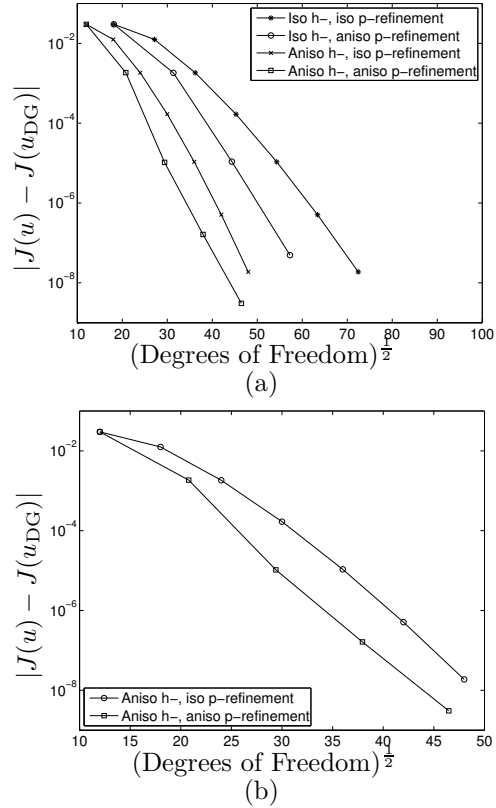


Figure 3: (a) Comparison between isotropic and anisotropic  $hp$ -mesh refinement algorithms for  $\varepsilon = 10^{-2}$ ; (b) Detail of (a) comparing only the algorithms based on employing anisotropic  $h$ -refinement.

ment, since the mesh resolution needed to adequately capture the boundary layers can be achieved with significantly less elements when the former strategy is employed. This behaviour becomes increasingly more evident the smaller  $\varepsilon$  is chosen. For a given mesh, we see that even employing a simple-minded anisotropic polynomial distribution still yields significant improvements in comparison to isotropic refinement of  $p$ ; indeed, here we observe that the former strategy leads to between one and two orders of magnitude improvement in the computed error in  $J(\cdot)$ , for a given number of degrees of freedom, compared with the latter approach.

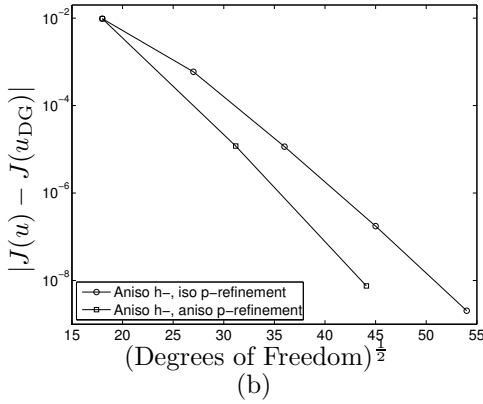
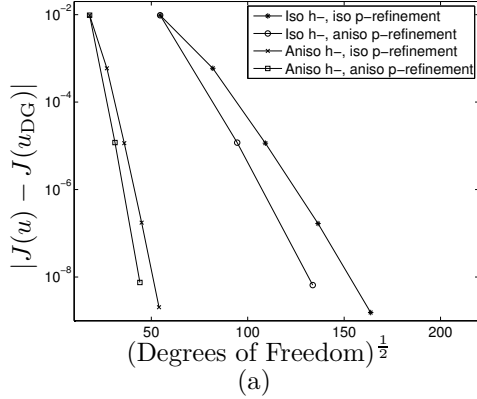


Figure 4: (a) Comparison between isotropic and anisotropic  $hp$ -mesh refinement algorithms for  $\varepsilon = 10^{-3}$ ; (b) Detail of (a) comparing only the algorithms based on employing anisotropic  $h$ -refinement.

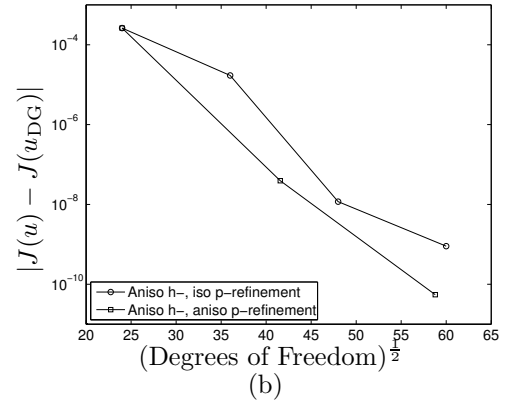
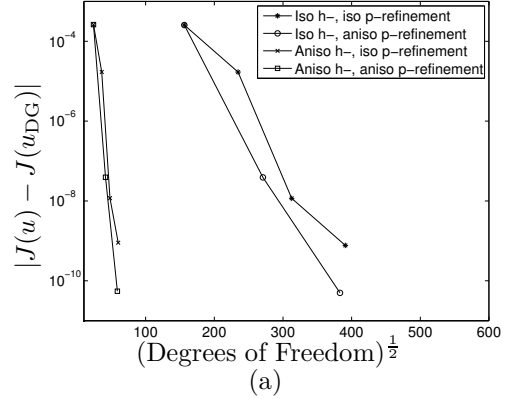


Figure 5: (a) Comparison between isotropic and anisotropic  $hp$ -mesh refinement algorithms for  $\varepsilon = 10^{-4}$ ; (b) Detail of (a) comparing only the algorithms based on employing anisotropic  $h$ -refinement.

## 6 Concluding remarks

In this article we have developed the *a priori* error analysis of  $hp$ -version interior penalty discontinuous Galerkin methods for second-order partial differential equations with nonnegative characteristic form in the goal-oriented setting, based on employing general finite element spaces incorporating both anisotropic computational meshes with anisotropic polynomial approximation degrees. Numerical experiments highlighting the potential benefits of employing such flexible finite element spaces have been presented based on *a priori* determining the anisotropy of both  $h$  and

$p$ . The development of an adaptive refinement strategy which can automatically choose the necessary anisotropy in both the computational mesh and polynomial degree distribution will be considered in the forthcoming companion paper [8].

## References

- [1] T. Apel. *Anisotropic finite elements: Local estimates and applications*. Advances in Numerical Mathematics, Teubner, Stuttgart, 1999.

- [2] R. Becker and R. Rannacher. Weighted a posteriori error control in FE methods. Technical report. Preprint 1, Interdisziplinäres Zentrum für Wissenschaftliches Rechnen, Universität Heidelberg, Heidelberg, Germany, 1996.
- [3] W. Cao. On the error of linear interpolation and the orientation, aspect ratio, and internal angles of a triangle. *SIAM J. Numer. Anal.*, 43(1):19–40, 2005.
- [4] L. Formaggia and S. Perotto. New anisotropic a priori error estimates. *Numer. Math.*, 89:641–667, 2001.
- [5] E.H. Georgoulis. Discontinuous Galerkin methods on shape-regular and anisotropic meshes. *D.Phil. Thesis*, University of Oxford, 2003.
- [6] E.H. Georgoulis.  $hp$ -version interior penalty discontinuous Galerkin finite element methods on anisotropic meshes. *Int. J. Numer. Anal. Model.*, 3:52–79, 2006.
- [7] E.H. Georgoulis, E. Hall, and P. Houston. Discontinuous Galerkin methods for advection–diffusion–reaction problems on anisotropically refined meshes. *Submitted for publication*.
- [8] E.H. Georgoulis, E. Hall, and P. Houston. Discontinuous Galerkin methods on  $hp$ -anisotropic meshes II: A posteriori error analysis and adaptivity. *In preparation*.
- [9] E.H. Georgoulis and A. Lasis. A note on the design of  $hp$ -version interior penalty discontinuous Galerkin finite element methods for degenerate problems. *IMA J. Numer. Anal.*, 26(2):381–390, 2006.
- [10] K. Harriman, P. Houston, B. Senior, and E. Süli.  $hp$ -Version discontinuous Galerkin methods with interior penalty for partial differential equations with nonnegative characteristic form. In C.-W. Shu, T. Tang, and S.-Y. Cheng, editors, *Recent Advances in Scientific Computing and Partial Differential Equations. Contemporary Mathematics Vol. 330*, pages 89–119. AMS, 2003.
- [11] P. Houston, C. Schwab, and E. Süli. Stabilized  $hp$ -finite element methods for first-order hyperbolic problems. *SIAM J. Numer. Anal.*, 37:1618–1643, 2000.
- [12] P. Houston, C. Schwab, and E. Süli. Discontinuous  $hp$ -finite element methods for advection–diffusion–reaction problems. *SIAM J. Numer. Anal.*, 39:2133–2163, 2002.
- [13] P. Houston and E. Süli.  $hp$ -Adaptive discontinuous Galerkin finite element methods for hyperbolic problems. *SIAM J. Sci. Comput.*, 23:1225–1251, 2001.
- [14] P. Houston and E. Süli. Stabilized  $hp$ -finite element approximation of partial differential equations with non-negative characteristic form. *Computing*, 66:99–119, 2001.
- [15] W. Huang. Mathematical principles of anisotropic mesh adaptation. *Commun. Comput. Phys.*, 1(2):276–310, 2006.
- [16] G. Kunert. *A posteriori error estimation for anisotropic tetrahedral and triangular finite element meshes*. PhD thesis, TU Chemnitz, 1999.
- [17] O.A. Oleinik and E.V. Radkevič. *Second Order Equations with Nonnegative Characteristic Form*. American Mathematical Society, Providence, R.I., 1973.
- [18] C. Schwab. *p- and hp-FEM – Theory and Application to Solid and Fluid Mechanics*. Oxford University Press, Oxford, 1998.
- [19] E. Süli, Ch. Schwab, and P. Houston.  $hp$ -DGFEM for partial differential equations with nonnegative characteristic form. In B. Cockburn, G.E. Karniadakis, and C.-W. Shu, editors, *Discontinuous Galerkin Methods: Theory, Computation and Applications, Lecture Notes in Computational Science and Engineering, Vol. 11*, pages 221–230. Springer, 2000.